ICARUS

INTERNATIONAL COOPERATION FOR SUSTAINABLE AVIATION BIOFUELS

D3.1 Technical assessment of selected SAFs

WP3: Assessments of cost-effectiveness and sustainability

March 2025

Tiago F. Lopes, Francisco Gírio

This project has received funding from the European Union's Horizon Europe research and innovation programme under grant agreement No. 101122303

Document History

Date	Version	Prepared by	Organisation	Approved by	Notes
04/02/2025	V1	Tiago Lopes	LNEG		Draft version
13/03/2025	V2	Francisco Gírio	LNEG		Revision
21/03/2025	V3	Niels Dögnitz, Max John Müller	DBFZ		Revision by WP3 partner
25/03/2025	V4	Tiago Lopes	LNEG		Final revision

Table 1: Document information

Document Information	
Project name:	ICARUS
Project title:	International cooperation for sustainable aviation biofuels
Project number:	101122303
Start date:	01/10/2023
Duration:	36 Months

Table 2: Dissemination level of this report

Dissemination level of this report	
PU	Public

ACKNOWLEDGMENT & DISCLAIMER

This project has received funding from the European Union's Horizon Europe research and innovation programme under grant agreement No 101122303.

Partners

Associated Partners

EXECUTIVE SUMMARY

This report focuses on the development and analysis of various sustainable aviation fuel (SAF) pathways to be implemented in the Aspen Plus® software. The report investigates multiple technological routes for producing SAF, evaluating their feasibility, efficiency and potential environmental impact.

The HEFA (Hydroprocessed Esters and Fatty Acids) pathway, FT (Fischer-Tropsch) pathway, AtJ (Alcohol-to-Jet) pathway and PtJ (Pyrolysis-to-Jet; or HTL-to-Jet) pathway are thoroughly reviewed, providing insights into their mechanisms and expected outcomes. Additionally, preliminary flowsheets for converting biocrude oils, isobutanol, and syngas to SAF are showcased, representing the initial models for further refinement.

The goal of this report is to establish robust and scalable processes for SAF production, which align with the European Union's sustainability and innovation objectives. This report serves as a crucial step towards achieving greener aviation, contributing to the overarching mission of reducing carbon emissions and fostering sustainable growth in the aviation sector.

Figures

Tables

Contents

1 Introduction

1.1 Background and objectives

The aviation sector is under increasing pressure to reduce its environmental impact, with sustainable aviation fuels (SAF) being recognized as a key strategy to achieve this goal (IATA, n.d.). Due to the urgency in mitigating greenhouse gas emissions (GHG) and the need for alternatives to fossil fuels, research and development of efficient and economically viable routes for SAF production has become a priority (ICAO, n.d.). This effort is driven by global regulatory initiatives, such as ICAO's Carbon Offsetting and Reduction Scheme for International Aviation (CORSIA), and targets set by entities like the International Energy Agency (IEA) and the European Union (EASA, n.d.; European Commission, n.d.). This report aims to explore various SAF production technologies reported in the literature, focusing on technical aspects, including process simulation. By providing an overview of the different pathways and technical considerations involved, this work seeks to support the development of more sustainable solutions for the aviation sector by offering preliminary flowsheets to be further implemented in Aspen Plus software, under the scope of Task 3.2.1 (Technical Analysis) of ICARUS project.

1.2 Overview of SAF production pathways

Sustainable Aviation Fuel (SAF) represents a pivotal innovation in the aviation industry, offering a pathway to significantly reduce greenhouse gas (GHG) emissions and advance environmental sustainability. To align with the CORSIA, SAF must meet stringent sustainability criteria that prioritize lifecycle GHG reductions, feedstock sustainability and compliance with environmental and social safeguards (Calderon et al., 2024; CORSIA, 2024). Among the diverse technological pathways for SAF production, three have emerged as particularly viable under CORSIA's framework: (i) Hydroprocessed Esters and Fatty Acids (HEFA), (ii) Fischer-Tropsch (FT), (iii) Alcohol-to-Jet (AtJ); and, currently under evaluation, (iv) Pyrolysis-to-Jet (PtJ). Their selection is grounded in their technical maturity, feedstock compatibility, and alignment with CORSIA's emissions reduction thresholds (minimum 10% lifecycle GHG reduction vs. conventional jet fuel, with many pathways exceeding 50%).

1.2.1 Hydroprocessed Esters and Fatty Acids (HEFA) pathway

The **HEFA pathway,** the most commercially advanced pathway, converts waste oils, fats, and greases into renewable jet fuel (Braun et al., 2024). CORSIA prioritizes this pathway due to its use of low-indirect land-use change (ILUC) risk feedstocks (e.g., used cooking oil, animal fats), which minimize competition with food production and reduce deforestation risks. HEFA also delivers high GHG savings (60–80% vs. fossil jet fuel), meeting CORSIA's stringent emissions benchmarks (CORSIA, 2024).

It involves the hydroprocessing of triglyceride feedstocks, such as vegetable oils, animal fats, and waste oils, to produce synthetic paraffinic kerosene (SPK). The key technical steps in the HEFA pathway include hydrotreating, which breaks down triglycerides into shorter hydrocarbon chains. The triglycerides are subjected to hydrogen in the presence of a catalyst, resulting in the removal of oxygen atoms and the formation of hydrocarbons. Hydroisomerization converts linear hydrocarbons into branched isomers to improve fuel properties. This step enhances the cold flow properties of the fuel, making it suitable for use in aviation. Hydrocracking further refines the hydrocarbon chains to meet jet fuel specifications. Hydrocracking breaks down larger molecules into smaller, more stable hydrocarbons, ensuring the fuel meets the required standards for energy content and combustion characteristics (Calderon et al., 2024). In (adapted from https://www.czapp.com/analyst-insights/hydrogens-crucial-role-in-saf-production/)

Figure 1 is represented the HEFA pathway to SAF.

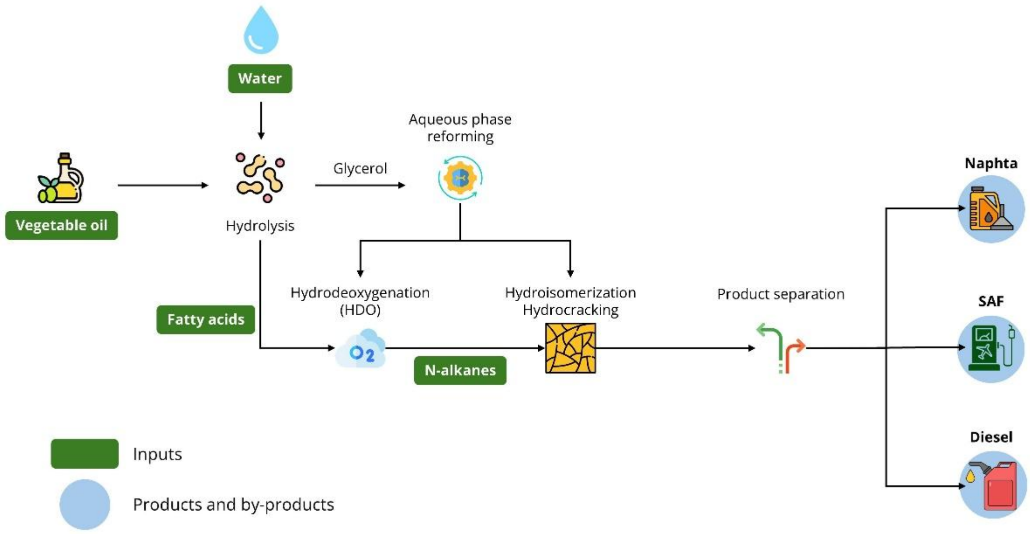

(adapted from https://www.czapp.com/analyst-insights/hydrogens-crucial-role-in-saf-production/)

Figure 1: The Hydroprocessed Esters and Fatty Acids (HEFA) pathway to SAF

1.2.2 Fischer-Tropsch pathway

The **Fischer-Tropsch (FT) pathway** synthesizes biomass, municipal solid waste (MSW) or agricultural residues into liquid fuels. Its inclusion under CORSIA stems from its ability to utilize lignocellulosic feedstocks (e.g., forestry residues), which are categorized as "advanced" under CORSIA's eligibility criteria. FT fuels achieve GHG reductions of 70–95%, depending on feedstock and energy inputs, and their high energy density ensures seamless integration with existing aircraft engines (CORSIA, 2024).

FT pathway utilizes gasification and synthesis gas (syngas) conversion to produce SAF. Biomass, MSW and other carbonaceous materials are gasified to generate syngas, which is then converted into liquid hydrocarbons through the FT synthesis. The technical aspects of the FT pathway include gasification, which converts feedstock into syngas, a mixture of carbon monoxide and hydrogen. This process involves heating the feedstock to high temperatures in the presence of a controlled amount of oxygen or steam. FT synthesis catalytically converts syngas into long-chain hydrocarbons, which are then refined into jet fuel. The FT synthesis uses a catalyst, typically iron or cobalt, to facilitate the chemical reactions that produce hydrocarbons suitable for aviation fuel (Calderon et al., 2024). In (adapted from https://www.czapp.com/analyst-insights/hydrogens-crucial-role-in-saf-production/)

Figure 2 is represented the FT pathway to SAF.

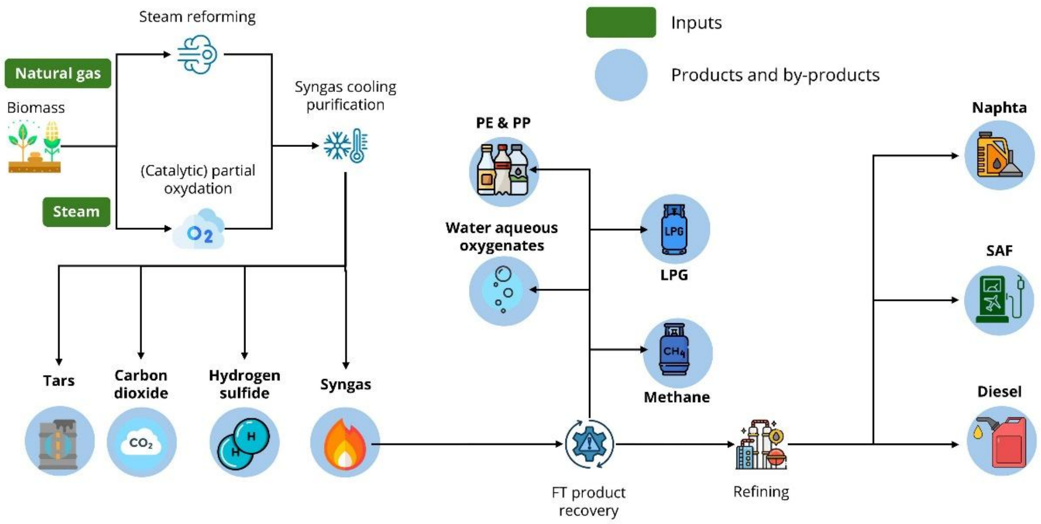

(adapted from https://www.czapp.com/analyst-insights/hydrogens-crucial-role-in-saf-production/)

Figure 2: The Fischer-Tropsch (FT) pathway to SAF

1.2.3 Alcohol-to-Jet pathway

The **Alcohol-to-Jet** (**AtJ) pathway** converts ethanol or isobutanol (derived from sugarcane, corn, or waste biomass) into jet fuel. CORSIA selectively approves AtJ pathways that employ residues or certified sustainable feedstocks to avoid food-versus-fuel conflicts. For instance, ethanol from agricultural residues can achieve ~70% GHG reductions, aligning with CORSIA's mid-term targets (CORSIA, 2024).

This process includes several key steps. Fermentation produces alcohol from biomass feedstocks like corn stover or sugarcane. Microorganisms are used to convert sugars into alcohol through fermentation. Dehydration removes water from the alcohol to produce olefins. This step involves the catalytic conversion of alcohols into olefins, which are unsaturated hydrocarbons. Oligomerization combines olefins into longer hydrocarbon chains. The olefins undergo polymerization reactions to form larger molecules suitable for jet fuel. Hydrotreatment refines the hydrocarbons to meet jet fuel specifications. Hydrotreatment involves the addition of hydrogen to the olefins, converting them into saturated hydrocarbons and removing impurities (Calderon et al., 2024). In Figure 3 is represented the AtJ pathway to SAF.

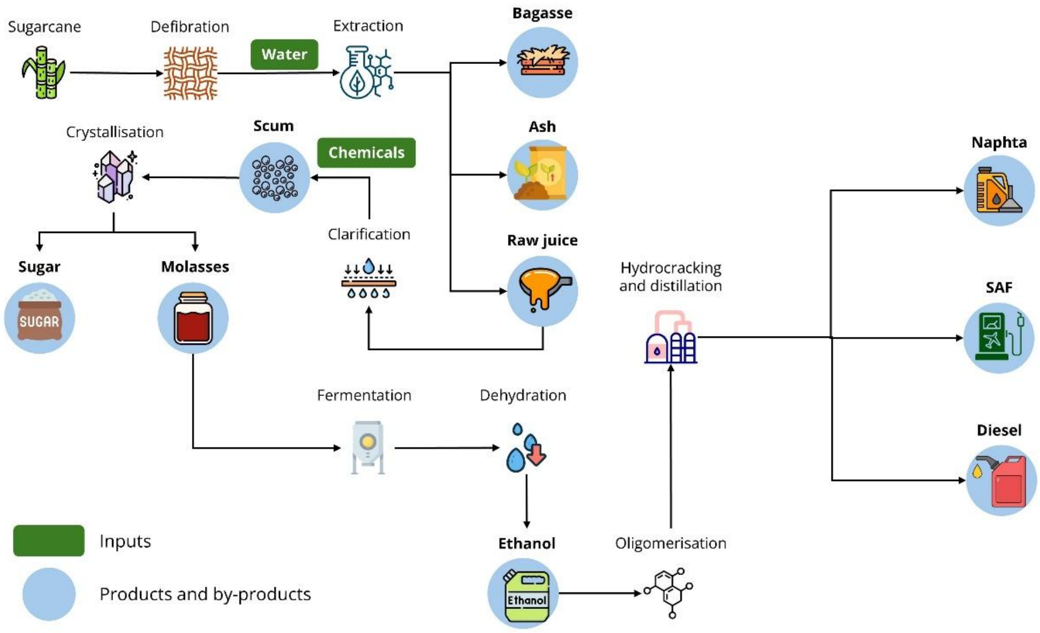

(adapted from https://www.czapp.com/analyst-insights/hydrogens-crucial-role-in-saf-production/)

Figure 3: The Alcohol-to-Jet (AtJ) pathway to SAF

1.2.4 Pyrolysis-to-Jet pathway

Although not yet ASTM-approved, the **Pyrolysis-to-Jet** (**PtJ) pathway** is an emerging technology that thermally decomposes agricultural or forestry waste into bio-oil, which is then upgraded to jet fuel. While less mature, PtJ is prioritized for its potential to utilize abundant, underutilized feedstocks (e.g., crop residues) with minimal ILUC impacts. Early assessments suggest it could achieve 50–80% GHG savings, contingent on sustainable feedstock sourcing and efficient processing (CORSIA, 2024).

At least three conversion processes using this approach are under evaluation (e.g., pyrolysis of non-recyclable plastics, biomass/waste pyrolysis) (ICAO, 2024). The bio-oil is then upgraded to jet fuel through hydrotreatment and other refining processes. The technical steps involved in the PTJ pathway include pyrolysis, which thermally decomposes biomass in the absence of oxygen to produce bio-oil. This process involves heating the biomass to high temperatures, causing it to break down into smaller molecules. Bio-oil collection involves condensing the volatile compounds generated during pyrolysis to form bio-oil, a complex mixture of oxygenated hydrocarbons, water, and other organic compounds. The bio-oil is separated from the syngas and char. Bio-oil stabilization is necessary because the raw bio-oil is highly reactive and unstable. Hydrotreatment is employed to stabilize the bio-oil by removing oxygenates and other reactive compounds. This process involves hydrodeoxygenation (HDO), a catalytic reaction where hydrogen is used to remove oxygen atoms from the bio-oil, converting oxygenated compounds into hydrocarbons. Hydrocracking breaks down larger molecules into smaller, more stable hydrocarbons. Catalytic upgrading involves selecting specific catalysts based on their ability to facilitate the conversion of bio-oil into desired hydrocarbon structures. Common catalysts include zeolites, noble metals, and metal oxides. Optimal temperature, pressure, and hydrogen flow rates are maintained to maximize the efficiency of catalytic upgrading. Fractionation involves subjecting the upgraded bio-oil to distillation to separate it into different fractions based on boiling points. This step isolates the jet fuel range hydrocarbons (typically C8 to C16) from other fractions like gasoline and diesel. Further purification processes, such as adsorption and filtration, are employed to remove any remaining impurities and ensure the fuel meets aviation standards. Blending and final refining involve blending the purified jet fuel fraction with conventional jet fuel (fossil Jet A) to meet ASTM D7566 specifications for SAF. This blending ensures compatibility with existing aircraft and fuel infrastructure. Rigorous testing and certification processes are conducted to verify that the final product meets all required specifications for aviation fuel, including energy content, freezing point, and combustion characteristics (Calderon et al., 2024). In Figure 4 is represented the PtJ pathway to SAF.

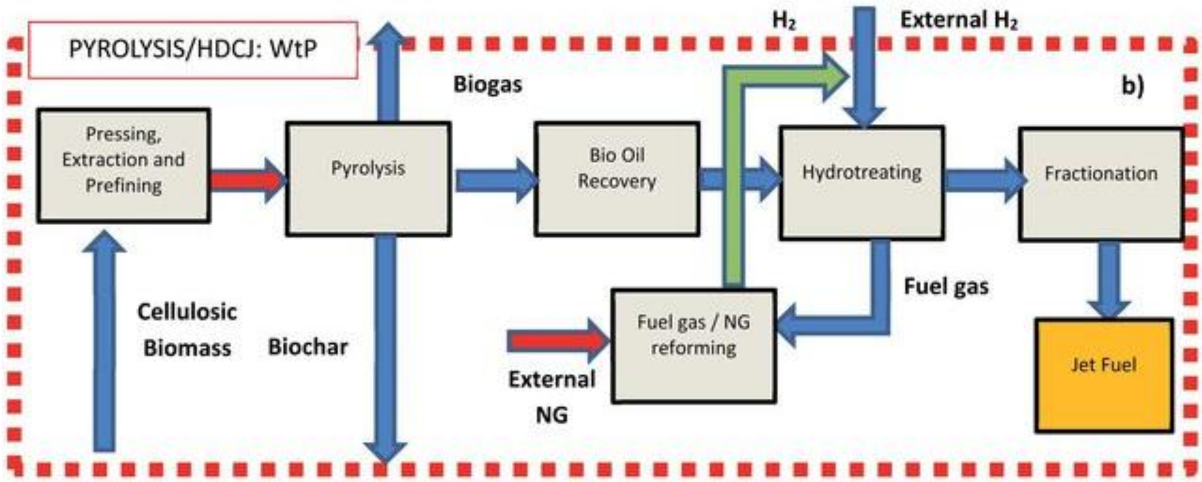

Source: (Kolosz et al., 2020)

Figure 4: The Pyrolysis-to-Jet (PtJ) pathway to SAF

1.2.5 General conclusions on available SAF pathways

CORSIA's framework incentivizes scalable, feedstock-flexible pathways that balance technical readiness with deep decarbonization. HEFA and FT are prioritized for their commercial viability and high GHG savings, while AtJ and PtJ are supported for their potential to diversify feedstock pools and address future scalability. Crucially, all four pathways adhere to CORSIA's requirement for independent sustainability certification, ensuring traceability from feedstock to final product. By focusing on these routes, the aviation sector can systematically reduce its reliance on fossil fuels while complying with CORSIA's evolving regulatory standards.

Each of these technological pathways offers unique advantages and challenges in the production of SAF. By leveraging diverse feedstocks and innovative conversion processes, these pathways contribute to the overarching goal of reducing aviation-related GHG emissions and achieving a sustainable future for air travel. As the industry continues to evolve, ongoing research and development will further enhance the efficiency and scalability of these SAF production technologies.

The selection of the most suitable production pathway depends on multiple factors, including the availability of feedstock, economic viability, technical aspects of the process and the environmental performance of the fuel produced (US Department of Energy, n.d.). Techno-economic analysis and life cycle assessment play a role in evaluating these different routes (see D3.2 and D3.3 for more details, respectively).

2 Scientific literature review

ICARUS project aims to develop SAF production routes through biocrude from hydrothermal liquefaction, isobutanol from lignocellulosic biomass and synthetic Fischer-Tropsch from biomass gasification. These value chains were selected for their proximity to market deployment and their necessity to meet European and international SAF deployment targets. The project addresses environmental impact, technological constraints, economic viability, and policy and legislation. It aims to improve SAF cost-effectiveness, facilitate scaling-up, and achieve global market deployment.

With a detailed focus on these value chains, the ICARUS project also strives to answer the research question (RQ) "How do process modelling and simulation contribute to the techno-economic and environmental assessment of different sustainable aviation fuel (SAF) production pathways from various feedstocks?". Thus, the search query employed in Web of Science™ was the following:

TS=(("sustainable aviation fuel*" OR "SAF") AND "process simulation")

With a time span from 2014 to 2025, yielding 15 records after the exclusion of unrelated works. This query targets contemporary scientific literature that incorporates process simulation in the investigation of SAF. Process simulation is an essential tool for the techno-economic and environmental evaluation of various SAF production pathways. It facilitates modelling and optimization of different conversion processes, estimation of costs, energy consumption and GHG emissions prior to large-scale implementation.

The following section discusses the key outcomes of these studies and their alignment with the primary objectives of the ICARUS project. The literature provides essential information for developing preliminary flowsheets, along with data obtained experimentally in Work Package 2 of ICARUS.

Further examination of the technical aspects of SAF pathways is available in D3.2.

2.1 Biocrude oils to SAF

The pathway of converting biocrude oils to SAF involves the use of lipidic feedstocks, such as vegetable oils, animal fats, algae oils, or pyrolytic oils derived from biomass, which are processed through technologies like hydrotreatment to produce hydrocarbons in the kerosene range. The hydrotreatment process (HEFA - Hydrotreated Esters and Fat Acids to Synthetic Paraffinic Kerosene) is one of the ASTM-certified routes and typically consists of two stages: the catalytic hydrogenation of the feedstock into free fatty acids and propane, followed by the conversion of fatty acids into long-chain paraffinic alkanes, CO2, and water through hydrodeoxygenation and decarboxylation. This process is promising in the short term, as it is already commercially available and has a high technology readiness level (TRL 9), also being used to produce HVO/green diesel (Monte et al., 2022).

The use of *Camelina sativa* oil as a feedstock for SAF production via hydrotreatment has been investigated, considering different process configurations for the valorisation of co-produced light gases (propane, methane, CO) to obtain hydrogen and/or energy needed in the process. The valorisation alternatives include steam reforming, autothermal reforming, and power generation through a combined cycle. The techno-economic analysis of these alternatives indicates that operating costs are dominated by the price of Camelina oil and strongly influenced by hydrogen and electricity prices (Monte et al., 2022).

The pyrolysis of biomass and waste, such as used tires, can also produce bio-oils that can be further refined into SAF through hydroprocessing. However, raw bio-oil generally requires additional refining to meet SAF standards due to the presence of oxygenates and other undesirable properties (Rogachuk & Okolie, 2024).

Hydrothermal liquefaction is another thermochemical process that can convert biomass into biocrude, which can be further processed into SAF (Seibel et al., 2024). Current assessments estimate the TRL of HTL for SAF production at 5-6, indicating a transition from pilot-scale validation to demonstration-phase systems, while the fuel readiness level (FRL) is not yet available(van Muijden et al., 2021).

Scientific literature has dedicated increasing attention to the production of SAF from vegetable oils and other lipidic feedstocks through hydrotreatment. Forest residues have also emerged as a significant feedstock, evaluated in recent years for the production of HTL bio-crude (Wijeyekoon et al., 2020). Studies like that of Martínez del Monte et al. (2022) present detailed techno-economic evaluations of different process configurations for SAF production from Camelina oil using process simulation (Monte et al., 2022). Other works explore the use of different catalysts in the hydrotreatment process to optimize the yield and quality of SAF. Patent analysis also reveals a trend of interest in the development of hydrotreatment processes for oily materials. Commercial technologies like UOP/ENI's Ecofining™ and Axens' Vegan™ are examples of well-established hydrotreatment processes for renewable feedstocks (Monte et al., 2022).

The comparison between different thermochemical processes, such as pyrolysis and gasification followed by Fischer-Tropsch, for the conversion of waste (like used tires) into SAF has been carried out, evaluating their economic and environmental impacts. These studies frequently use process simulation to model the different stages and life cycle assessment (LCA) to quantify environmental impacts (Rogachuk & Okolie, 2024).

2.2 Isobutanol to SAF

The pathway for SAF production from isobutanol (and other alcohols like ethanol) is known as Alcohol-to-Jet (ATJ). This pathway involves a series of catalytic reactions, including alcohol dehydration to produce olefins, olefin oligomerization to form longer-chain hydrocarbons in the SAF range, and finally, hydrogenation to saturate the unsaturated bonds. Isobutanol, like ethanol, can be produced from the fermentation of sugars derived from lignocellulosic biomass, such as agricultural residues, wood chips, and grasses (Geleynse et al., 2018; Teixeira et al., 2024).

One of the advantages of this pathway is the possibility of using existing first-generation biorefinery infrastructures for alcohol production, which can be further converted into SAF. However, the purification of alcohol by energy-intensive distillation and the dehydration step increase complexity and can reduce the process's sustainability (Teixeira et al., 2024).

Studies have evaluated the techno-economic feasibility of SAF production from ethanol, considering different process configurations and economic scenarios. The integration of ethanol production from steel industry waste gases, followed by conversion to SAF (ETJ), has also been investigated, demonstrating potential for greenhouse gas emission reduction (Wang et al., 2023).

Scientific literature includes studies that explore the optimization of the ATJ process, techno-economic evaluation of different configurations, and life cycle analysis to quantify environmental impacts. Teixeira et al. (2024) simulated the ATJ process for biojet fuel production from ethanol in the Brazilian context and estimated breakeven prices (Teixeira et al., 2024). Petersen et al. (2021) conducted comprehensive comparisons of different refinery configurations for SAF production from bioethanol, using process simulation and techno-economic assessment (Petersen et al., 2021). Other studies focus on the intensification of the ATJ process to improve efficiency and reduce costs (Teixeira et al., 2024). Life cycle assessment of SAF production from ethanol from different biomass sources has also been carried out to determine the potential for greenhouse gas emission reduction. Machine learning-based frameworks are also being explored to estimate techno-economic uncertainty in biofuel production pathways, including ATJ (Wu et al., 2024).

2.3 Syngas to SAF

The pathway for SAF production from synthesis gas (syngas) involves the gasification of lignocellulosic biomass, municipal solid waste, or other carbonaceous feedstocks to produce a gas composed mainly of carbon monoxide (CO) and hydrogen (H_2). The syngas is then converted into liquid hydrocarbons, including SAF, through Fischer-Tropsch (FT) synthesis. The FT process uses catalysts (such as cobalt, iron, nickel, or ruthenium) to catalyze the polymerization of CO and H_2 into long-chain hydrocarbons, which are subsequently fractionated and upgraded (for example, through hydrocracking, isomerization, and aromatization) to obtain SAF that meets the necessary specifications (Lan et al., 2024). Biomass gasification can be integrated with existing infrastructure, such as sugarcane biorefineries, to improve the economic viability of SAF production. The use of biomass densification methods, such as fast pyrolysis, can reduce the transportation costs of the feedstock to the gasification and FT units (Bube et al., 2024).

The production of syngas from steel industry waste gases, namely Basic Oxygen Furnace Gas (BOFG) and Coke Oven Gas (COG), has also been explored as a route for SAF production via FTJ (Fischer-Tropsch to Jet fuel), demonstrating significant potential for reducing greenhouse gas emissions compared to traditional aviation fuels. E-fuels, produced from renewable hydrogen and captured carbon dioxide, also utilize syngas as an intermediate for e-kerosene production via Fischer-Tropsch synthesis (Guo et al., 2024).

Scientific literature addresses various aspects of SAF production from syngas, including the development of more efficient and selective FT catalysts, optimization of process conditions, techno-economic evaluation of different process configurations, and life cycle analysis to quantify environmental impacts. Studies like that of Guimarães et al. (2023) present techno-economic and environmental assessments of biomass gasification and Fischer-Tropsch synthesis integrated into sugarcane biorefineries (Real Guimarães et al., 2023). The use of syngas derived from the catalytic reforming of refined biogas has also been evaluated for SAF production. The integration of pyrolysis units for bio-oil production, followed by steam reforming for hydrogen/syngas production, is also considered (Lan et al., 2024). Research also extends to the use of CO2 as a feedstock for syngas production for Fischer-Tropsch synthesis. Process simulation plays a crucial role in these studies, allowing for the modelling and optimization of gasification and FT synthesis units (Lan et al., 2024).

2.4 Sustainable Aviation Fuel Production Pathways: Process Simulation and Assessment

The following Table 3 provides a comprehensive summary of the various Sustainable Aviation Fuel (SAF) production pathways, reported in the literature, that have been evaluated through process simulation. The table highlights key aspects of these pathways, including the type of feedstock used, the geographical location of the studies, the specific processes involved, and the software tools utilized for simulation. Additionally, techno-economic assessments (TEA), life cycle assessments (LCA), carbon efficiency and energy efficiency metrics are presented to offer a detailed comparison of the sustainability and feasibility of different SAF production methods.

Table 3: Literature-based summary of Sustainable Aviation Fuel (SAF) production pathways that report process simulation

Feedstock	Location	Process	Process Simulation	Software	TEA	LCA	Reference
Ethanol (from corn)	Brazil	Alcohol-to-Jet (ATJ)	Yes	Aspen Plus® v12.1	Yes	No	(Teixeira et al., 2024)
Ethanol (from corn stover)	Brazil	Alcohol-to-Jet (ATJ)	Yes	Aspen Plus® v12.1	Yes	No	(Teixeira et al., 2024)
Basic Oxygen Furnace Gas (BOFG)	China	Ethanol-to-Jet (ETJ)	Yes	Aspen Plus® (V11)	No	Yes	(Guo et al., 2024)
Basic Oxygen Furnace Gas (BOFG)	China	Fischer-Tropsch to Jet (FTJ)	Yes	Aspen Plus® (V11)	No	Yes	(Guo et al., 2024)
Coke Oven Gas (COG)	China	Ethanol-to-Jet (ETJ)	Yes	Aspen Plus® (V11)	No	Yes	(Guo et al., 2024)
Coke Oven Gas (COG)	China	Fischer-Tropsch to Jet (FTJ)	Yes	Aspen Plus® (V11)	No	Yes	(Guo et al., 2024)
(COG + BOFG)	China	Ethanol-to-Jet (ETJ)	Yes	Aspen Plus® (V11)	No	Yes	(Guo et al., 2024)

(COG + BOFG)	China	Fischer-Tropsch to Jet (FTJ)	Yes	Aspen Plus® (V11)	No	Yes	(Guo et al., 2024)
Lignocellulosic Biomass (sugarcane bagasse and straw)	Brazil	Gasification and Fischer-Tropsch synthesis (GFT)	Yes	Aspen Plus® (V 9.0)	Yes	Yes	(Real Guimarães et al., 2023)
Camelina Oil	Spain	Hydrotreatment and hydrocracking	Yes	Aspen Plus®	Yes	Yes	(Monte et al., 2022)
Corn	USA	Conversion to 1,4-dimethylcyclooctane (DMCO)	Yes	Not specified	No	Yes	(Batten et al., 2023)
Biogas and Corn Stover	Not specified	Hybrid biogas-to-kerosene process	Yes	Aspen Plus® (V12)	Yes	No	(Voß et al., 2024)
Tall Oil Fatty Acid (TOFA)	Not specified	Catalytic deoxygenation (decarboxylation/decarbonylation)	Yes	Aspen Plus®	Yes	Yes	(Umenweke et al., 2023)
Tall Oil Fatty Acid (TOFA)	Not specified	Catalytic deoxygenation integrated with hydrothermal gasification for H_2	Yes	Aspen Plus®	Yes	Yes	(Umenweke et al., 2023)
Paper Sludge	USA	Enzymatic hydrolysis, dehydration, aldol condensation, hydroprocessing	Yes	Aspen Plus® (V11)	No	Yes	(Lan et al., 2024)

Used Tires	Not specified	Pyrolysis	Yes	Aspen Plus®	Yes	Yes	(Rogachuk & Okolie, 2024)
Soybean Oil and Animal Tallow	Brazil	Hydrotreatment (deoxygenation, isomerization, hydrocracking)	Yes	UniSim Design R491	Yes	Yes	(Teixeira et al., 2024)

3 Process design and optimization

The objective of this section is to suggest preliminary flowsheets to be applied to the selected Sustainable Aviation Fuel (SAF) pathways in ICARUS project. By developing and optimizing these process designs, we aim to enhance the conversion efficiency of various feedstocks into SAF. The following subsections outline the specific pathways and corresponding flowsheets to be implemented in the Aspen Plus® software.

3.1 Process Flowsheets

In the quest for sustainable aviation fuels (SAF), it is imperative to explore and optimize various pathways for converting diverse feedstocks into viable fuel alternatives. In this section, we delve into the process design and optimization strategies employed to achieve efficient conversion and high yield of SAF. The pathways discussed herein are implemented using the Aspen Plus® software, which serves as a robust platform for modelling, simulation and analysis of chemical processes. Our objective is to lay the groundwork for developing comprehensive flowsheets that enhance the technical and economic feasibility of SAF production.

This section presents preliminary flowsheets for three distinct pathways: biocrude oils, isobutanol and syngas, each representing a unique approach to SAF synthesis. By examining these pathways, we aim to identify key process parameters, optimize conversion efficiencies, and address potential challenges in the simulation framework. This preliminary model implementation in Aspen Plus® serves as a foundational step in the ICARUS project. It provides a basis for understanding the technical and economic aspects of SAF production from different feedstocks. Over the following months, these models will be refined and consolidated to develop comprehensive and optimized process designs that can be scaled up for industrial application.

Furthermore, the flowsheets may be adjusted during model development and by integrating feedback from partners involved in the technical Work Packages.

3.1.1 Biocrude oils to SAF

Biocrude oil conversion to SAF involves a multi-step process that begins with the extraction of biocrude oils from various biomass sources. Specifically, for ICARUS project, microalgal biomass was selected as the most adequate feedstock for this pathway. The oils obtained from the hydrothermal liquefaction (HTL) of this biomass undergo a series of chemical reactions, including hydrotreating and hydrocracking, to produce high-quality jet fuel. The preliminary flowsheet for this pathway, represented in Figure 5, outlines the key stages of the conversion process, detailing the catalysts, reaction conditions and separation techniques employed.

The flowsheet is divided into two main sections:

(i) Cultivation and harvesting of microalgae: Microalgae are grown in raceways or photobioreactors using wastewater, then harvested and submitted to a solid-liquid separation with membranes or centrifugation.

(ii) HTL and bio-oil upgrading to SAF: Microalgae is harvested, processed in the HTL reactor for bio-oil production and then refined to SAF.

For the process simulation, the cultivation and harvesting steps are not included – although will be considered for the environmental analysis of this pathway due to the carbon uptake. Subsequently, the algal biomass is subjected to HTL producing apart from bio-oil, also biochar, gases and an aqueous phase. Then, the upgrading of biocrude oils involves processes such as deoxygenation, where oxygen-containing compounds are removed, and hydrogenation, which saturates the hydrocarbon chains. The remaining downstream section covers the refining steps, where the upgraded biocrude undergoes cracking and distillation to produce the final SAF product. The process simulation will consider various parameters, including feedstock variability (namely its CHNSO composition), catalyst performance, and energy integration, to optimize the overall efficiency and yield of the SAF production.

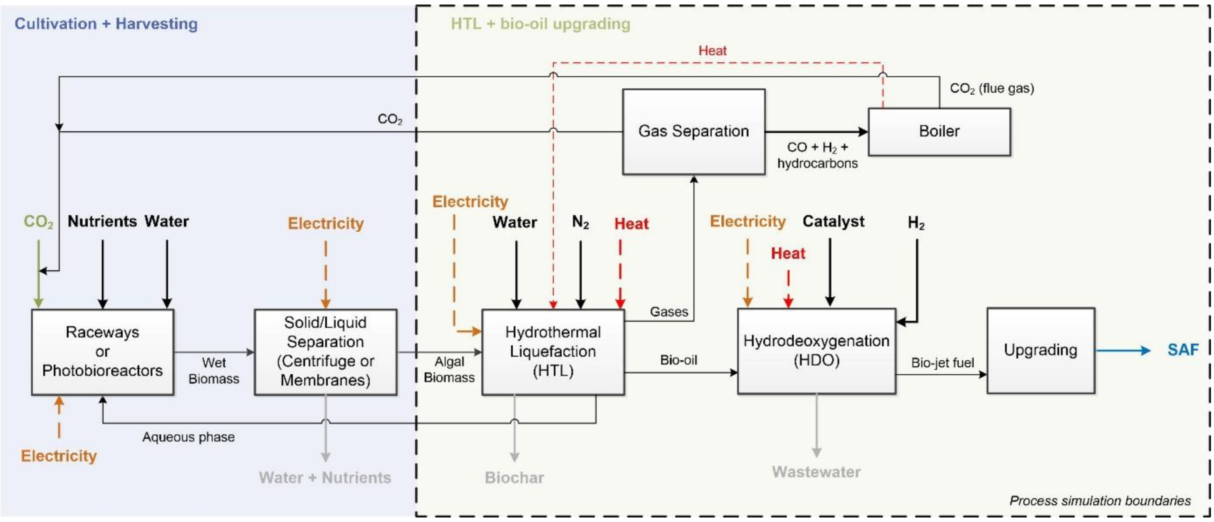

Figure 5: Preliminary flowsheet of biocrude oils to SAF pathway to be implemented in Aspen Plus® software

3.1.2 Isobutanol to SAF

The pathway for converting isobutanol to sustainable aviation fuel (SAF) encompasses a series of carefully designed processes aimed at transforming biomass-derived sugars into high-quality jet fuel, following the AtJ approach. The preliminary flowsheet, depicted in Figure 6, outlines the critical stages involved in this conversion, emphasizing the importance of each step in achieving optimal fuel yield and efficiency. The process model will be developed in two stages – the first one will focus on the isobutanol conversion to SAF, while the second will include the fermentation to isobutanol.

The flowsheet is divided into two primary sections:

(i) The production of isobutanol from biomass sugars: This involves the fermentation of biomass sugars to produce isobutanol. The fermentation step is crucial for obtaining a consistent and high yield of isobutanol, which serves as the cornerstone for subsequent fuel synthesis. This step will be considered in the 2nd stage of the model development.

(ii) The conversion of isobutanol to SAF: The isobutanol is then subjected to dehydration and oligomerization processes to form jet fuel range hydrocarbons. This section covers the chemical transformations required to upgrade isobutanol into a viable aviation fuel, focusing on reaction conditions, catalyst selection and separation techniques. This step will be considered in the 1st stage of the model development.

In the process simulation, various factors will be carefully considered to optimize the overall efficiency and yield of the SAF production. These include fermentation to isobutanol efficiency (to be assessed in the 2nd stage of the model development), the performance of catalysts for SAF-range olefins and the hydrocarbon chain length distribution. By starting the model implementation with isobutanol as the initial feedstock, the simulation aims to provide a robust framework that can be refined and scaled up for industrial application over the following months of the ICARUS project.

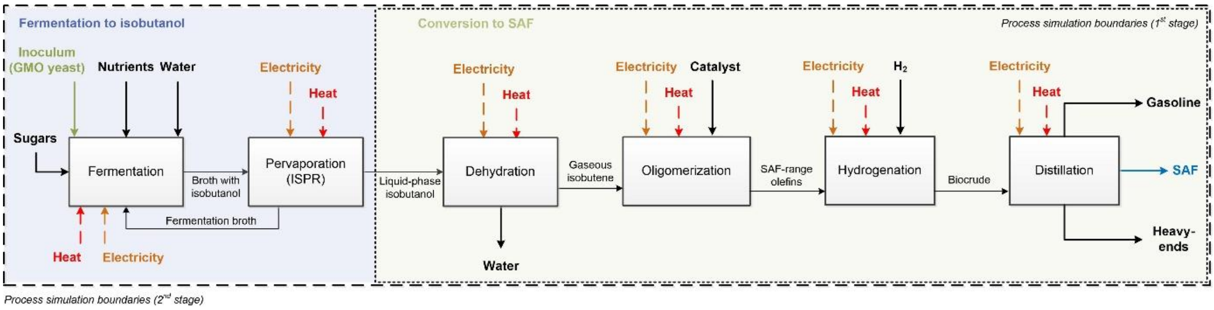

Figure 6: Preliminary flowsheet of isobutanol to SAF pathway to be implemented in Aspen Plus® software

3.1.3 Syngas to SAF

Syngas, a versatile mixture of carbon monoxide and hydrogen, represents a pivotal intermediary in the conversion of various feedstocks such as biomass, waste and natural gas into sustainable aviation fuel (SAF). The preliminary model implementation outlined in Figure 7 focuses on the intricate processes aimed at achieving this transformation efficiently and sustainably.

The flowsheet for the syngas to SAF pathway is methodically divided into two primary sections:

- Syngas production: This section encompasses the generation of syngas from various feedstocks. Although essential, the syngas production stage will not be included in the initial model implementation due to its well-established nature in both literature and industry. The emphasis will be on the subsequent stages to streamline the development process.
- Syngas conversion to SAF through the Fischer-Tropsch (FT) pathway: In this section, syngas undergoes catalytic conversion via the Fischer-Tropsch synthesis, producing a diverse mixture of hydrocarbons. These hydrocarbons are then subjected to hydrocracking and distillation processes to yield high-quality jet fuel. The process simulation in this stage will consider factors such as syngas composition, catalyst selection and reactor configuration to optimize the SAF yield and quality.

As we venture into the preliminary model implementation of the syngas to SAF pathway, it is imperative to note that this is an initial framework intended to lay the groundwork for more comprehensive and refined models. The consolidated model will be developed over the following months, incorporating intricate details and optimizations based on the outcomes of ongoing simulations and research.

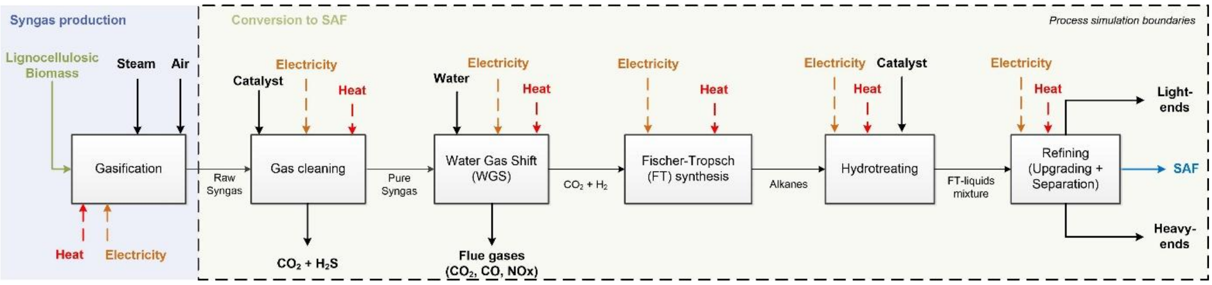

Figure 7: Preliminary flowsheet of syngas to SAF pathway to be implemented in Aspen Plus® software

3.2 Preliminary model implementation in Aspen Plus®

The following section aims to report the status of the development of the models for the three ICARUS pathways: Isobutanol to SAF, Syngas to SAF and Biocrude oils to SAF. It is important to note that the models presented are preliminary frameworks. The consolidated models will be developed over the upcoming months of the ICARUS project. Continuous research and detailed simulations will further refine and optimize these frameworks to achieve efficient and sustainable fuel production.

3.2.1 Biocrude oils to SAF

Figure 8 depicts an example of the preliminary model implemented in Aspen Plus® for the biocrude oils to SAF pathway. It contains data from literature for microalgae cultivated in wastewater. A more detailed version (that includes the bio-oil upgrading) can be found in the Appendix. The HTL reactor is defined based on kinetics, allowing the model to be flexible for using different feedstocks. This approach ensures the model can adapt to various sources of biocrude, providing a versatile framework for future developments.

Although the biocrude upgrade was tested, it has not yet been optimized. This upgrade process is crucial as it aims to improve the quality of biocrude oil, making it more suitable for conversion into SAF. The optimization will involve refining the process parameters to enhance yield and quality, incorporating insights from ongoing research and simulations.

What is represented in the figure includes the obtention of biocrude, biochar and the aqueous phase from HTL. Biochar is a valuable co-product that can be used for soil amendment and carbon sequestration, while the aqueous phase contains valuable nutrients that could potentially be recycled, treated or converted to higher value products, such as fuels and/or chemicals (Zhu et al., 2019). Other authors suggest its use as an acid for the microalgae pretreatment prior to HTL (Mahima et al., 2021).

The figure also includes heat demand (Q in blue for heat exchangers and reactors), pump power (W) and the total mass balances for each stream. Additional details can be found in Appendix. Heat demand is a critical factor in the process as it affects the overall energy efficiency and sustainability of the conversion pathway. The total mass balances provide a detailed overview of the flow of materials through the system, ensuring that all input and output streams are accounted for. Additionally, the model presents the stream conditions (pressure and temperature).

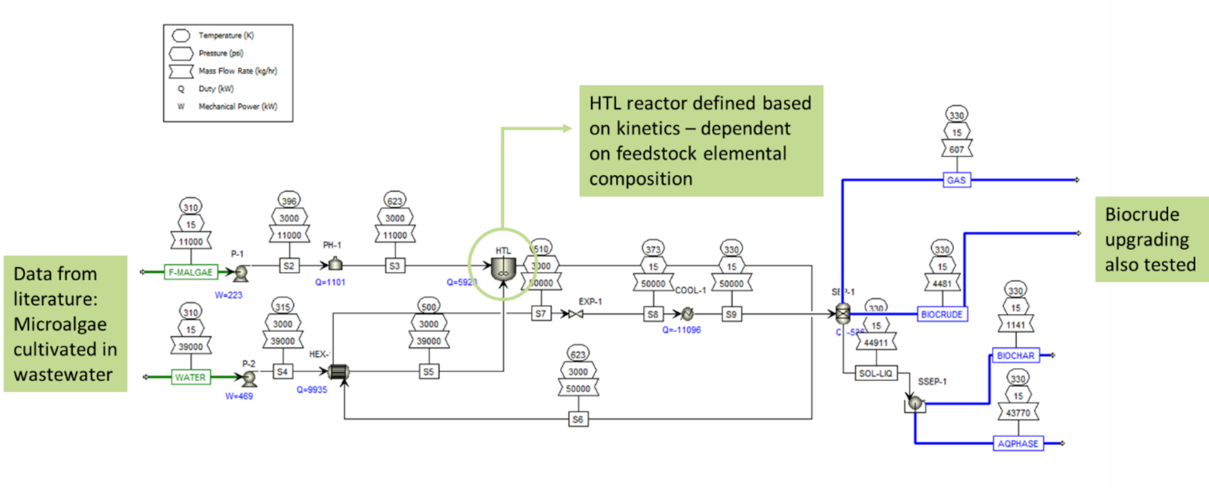

Figure 8: Preliminary model implemented in Aspen Plus® software for biocrude oils to SAF pathway

3.2.2 Isobutanol to SAF

The isobutanol to SAF pathway is currently in development stage, with various aspects being optimized to ensure efficient and sustainable fuel production. The energy and mass balances will be made available at the end of Task 3.2.1 (D3.6).

3.2.3 Syngas to SAF

The syngas to SAF pathway will be developed at a later stage as it is more well-established in both literature and industry. The energy and mass balances will be made available at the end of Task 3.2.1 (D3.6).

4 Conclusions

The preliminary models created in Aspen Plus® for converting biocrude oils to SAF look promising for energy efficiency and sustainability. Including heat demands and total mass balances gives a clear picture of energy use and material flow, which is crucial for optimizing the process and the economic (see D3.2 for more details) and environmental (see D3.3 for more details) analysis of the selected pathways.

The ongoing work on the isobutanol to SAF pathway (Task 3.2.1) aims to refine the energy and mass balances for efficient fuel production. The syngas to SAF pathway, while scheduled for later development, already has well-established methods in literature and industry.

Overall, the models and flowsheets from this study provide a flexible framework for SAF production from various feedstocks. These efforts are key to achieving SAF production targets and boosting the sustainability of aviation fuels. Continued research and development in this area are vital for reducing the aviation industry's carbon footprint and achieving broader environmental goals.

5 References

Batten, R., Galant, O., Karanjikar, M., & Spatari, S. (2023). Meeting sustainable aviation fuel policy targets through first generation corn biorefineries. *Fuel*, *333*, 126294. https://doi.org/10.1016/j.fuel.2022.126294

Braun, M., Grimme, W., & Oesingmann, K. (2024). Pathway to net zero: Reviewing sustainable aviation fuels, environmental impacts and pricing. *Journal of Air Transport Management*, *117*, 102580. https://doi.org/10.1016/J.JAIRTRAMAN.2024.102580

Bube, S., Bullerdiek, N., Voß, S., & Kaltschmitt, M. (2024). Kerosene production from power-based syngas – A technical comparison of the Fischer-Tropsch and methanol pathway. *Fuel*, *366*. https://doi.org/10.1016/j.fuel.2024.131269

Calderon, O. R., Tao, L., Abdullah, Z., Moriarty, K., Smolinski, S., Milbrandt, A., Talmadge, M., Bhatt, A., Zhang, Y., Ravi, V., Skangos, C., Tan, E., & Payne, C. (2024). *Sustainable Aviation Fuel (SAF) State-of-Industry Report: State of SAF Production Process*. https://www.nrel.gov/docs/fy24osti/87802.pdf

CORSIA. (2024). *CORSIA Eligible Fuels*. https://www.icao.int/environmental-protection/CORSIA/Pages/CORSIA-Eligible-Fuels.aspx

EASA. (n.d.). *Carbon Offsetting and Reduction Scheme for International Aviation (CORSIA)*. Retrieved March 12, 2025, from https://www.easa.europa.eu/en/domains/environment/eaer/market-based-measures/carbon-offsetting-and-reduction-scheme-international

European Commission. (n.d.). *Reducing emissions from aviation*. Retrieved March 12, 2025, from https://climate.ec.europa.eu/eu-action/transport/reducing-emissions-aviation_en

Geleynse, S., Brandt, K., Garcia-Perez, M., Wolcott, M., & Zhang, X. (2018). The Alcohol-to-Jet Conversion Pathway for Drop-In Biofuels: Techno-Economic Evaluation. *ChemSusChem*, *11*(21), 3728–3741. https://doi.org/10.1002/cssc.201801690

Guo, L., Wang, X., Yang, W., & Lv, J. (2024). Life Cycle Assessment of Aviation Fuel Production from Steel-Industry Off-Gas. *Processes*, *12*(3), 579. https://doi.org/10.3390/pr12030579

IATA. (n.d.). *Developing Sustainable Aviation Fuel (SAF)*. Retrieved March 12, 2025, from https://www.iata.org/en/programs/sustainability/sustainable-aviation-fuels/#tab-1

ICAO. (n.d.). *Sustainable Aviation Fuels (SAF)* . Retrieved March 12, 2025, from https://www.icao.int/environmental-protection/pages/SAF.aspx

ICAO. (2024). *Conversion processes under evaluation*. https://www.icao.int/environmental-protection/GFAAF/Pages/conversion-processes.aspx

Kolosz, B. W., Luo, Y., Xu, B., Maroto-Valer, M. M., & Andresen, J. M. (2020). Life cycle environmental analysis of "drop in" alternative aviation fuels: A review. In *Sustainable Energy and Fuels* (Vol. 4, Issue 7, pp. 3229–3263). Royal Society of Chemistry. https://doi.org/10.1039/c9se00788a

Lan, K., Cruz, D., Li, J., Agyei Boakye, A. A., Park, H., Tiller, P., Mittal, A., Johnson, D. K., Park, S., & Yao, Y. (2024). Life-Cycle Assessment of Sustainable Aviation Fuel Derived from Paper Sludge. *ACS Sustainable Chemistry & Engineering*, *12*(22), 8379–8390. https://doi.org/10.1021/acssuschemeng.4c00795

Mahima, J., Sundaresh, R. K., Gopinath, K. P., Rajan, P. S. S., Arun, J., Kim, S. H., & Pugazhendhi, A. (2021). Effect of algae (Scenedesmus obliquus) biomass pre-treatment on bio-oil production in hydrothermal liquefaction (HTL): Biochar and aqueous phase utilization studies. *Science of The Total Environment*, *778*, 146262. https://doi.org/10.1016/J.SCITOTENV.2021.146262

Monte, D. M. del, Cruz, P. L., & Dufour, J. (2022). SAF production from cameline oil hydrotreatment: A technoeconomic assessment of alternative process configurations. *Fuel*, *324*, 124602. https://doi.org/10.1016/j.fuel.2022.124602

Petersen, A. M., Chireshe, F., Okoro, O., Gorgens, J., & Van Dyk, J. (2021). Evaluating refinery configurations for deriving sustainable aviation fuel from ethanol or syncrude. *Fuel Processing Technology*, *219*, 106879. https://doi.org/10.1016/j.fuproc.2021.106879

Real Guimarães, H., Marcon Bressanin, J., Lopes Motta, I., Ferreira Chagas, M., Colling Klein, B., Bonomi, A., Maciel Filho, R., & Djun Barbosa Watanabe, M. (2023). Decentralization of sustainable aviation fuel production in Brazil through Biomass-to-Liquids routes: A techno-economic and environmental evaluation. *Energy Conversion and Management*, *276*, 116547. https://doi.org/10.1016/j.enconman.2022.116547

Rogachuk, B. E., & Okolie, J. A. (2024). Comparative assessment of pyrolysis and Gasification-Fischer Tropsch for sustainable aviation fuel production from waste tires. *Energy Conversion and Management*, *302*, 118110. https://doi.org/10.1016/j.enconman.2024.118110

Seibel, J., Cabral Wancura, J. H., & Dias Mayer, F. (2024). Process simulation and technology prospection to the hydrotreating of vegetable oils and animal fats. *Energy Conversion and Management*, *315*, 118811. https://doi.org/10.1016/j.enconman.2024.118811

Teixeira, A. T., da Silva, A. C. M., Cavalcante, R. M., & Young, A. F. (2024). Process simulation and economic evaluation of the Alcohol-to-Jet production of sustainable aviation fuel in the Brazilian context. *Energy Conversion and Management*, *319*, 118947. https://doi.org/10.1016/j.enconman.2024.118947

Umenweke, G. C., Pace, R. B., Santillan-Jimenez, E., & Okolie, J. A. (2023). Techno-economic and life-cycle analyses of sustainable aviation fuel production via integrated catalytic deoxygenation and hydrothermal gasification. *Chemical Engineering Journal*, *452*, 139215. https://doi.org/10.1016/j.cej.2022.139215

US Department of Energy. (n.d.). *Sustainable Aviation Fuel*. Alternative Fuels Data Center. Retrieved March 12, 2025, from https://afdc.energy.gov/fuels/sustainable-aviation-fuel?utm=syndication

van Muijden, J., Stepchuk, I. ;, de Boer, A. I. ;, Kogenhop, O. ;, Rademaker, E. R. ;, van der Sman, E. S. ;, Kos, J. ;, Posada Duque, J. A. ;, & Palmeros Parada, M. D. M. (2021). *Final results alternative energy and propulsion technology literature study*. https://cordis.europa.eu/project/id/864089/results

Voß, S., Bube, S., & Kaltschmitt, M. (2024). Hybrid Biomass- and Electricity-Based Kerosene Production—A Techno-Economic Analysis. *Energy & Fuels*, *38*(6), 5263–5278. https://doi.org/10.1021/acs.energyfuels.3c04876

Wang, X., Guo, L., Lv, J., Li, M., Huang, S., Wang, Y., & Ma, X. (2023). Process design, modeling and life cycle analysis of energy consumption and GHG emission for jet fuel production from bioethanol in China. *Journal of Cleaner Production*, *389*, 136027. https://doi.org/10.1016/j.jclepro.2023.136027

Wijeyekoon, S., Torr, K., Corkan, H., & Bennet, P. (2020). *Commercial status of direct thermochemical liquefaction technologies* .

Wu, C., Wang, Y., & Tao, L. (2024). Machine learning-enabled techno-economic uncertainty analysis of sustainable aviation fuel production pathways. *Chemical Engineering Journal Advances*, *20*, 100650. https://doi.org/10.1016/j.ceja.2024.100650

Zhu, Y., Jones, S. B., Schmidt, A. J., Albrecht, K. O., Edmundson, S. J., & Anderson, D. B. (2019). Techno-economic analysis of alternative aqueous phase treatment methods for microalgae hydrothermal liquefaction and biocrude upgrading system. *Algal Research*, *39*, 101467. https://doi.org/10.1016/J.ALGAL.2019.101467

6 Appendix

Table A 1: Literature-based summary of Sustainable Aviation Fuel (SAF) production pathways that report process simulation (complete table)

Feedstock	Location	Process	Process Simulation	Software	TEA	LCA	Carbon Efficiency	Energy Efficiency	Production Cost	Reference
Camelina Oil	Spain	Hydrotreatment and hydrocracking	Yes	Aspen Plus®	Yes	Yes	29.9%	24.3%	2.77 €/kg jetfuel	(Monte et al., 2022)
Corn	USA	Conversion to 1,4-dimethylcyclooctane (DMCO)	Yes	Not specified	No	Yes	36 g CO_2e/MJ DMCO (base case) 5 g CO_2e/MJ DMCO (with CCS)	Not specified	Not specified	(Batten et al., 2023)
Lignocellulosic Biomass (sugarcane bagasse and straw)	Brazil	Gasification and Fischer-Tropsch synthesis (GFT)	Yes	Aspen Plus® (V 9.0)	Yes	Yes	~80 g CO_2 eq avoided/MJ SAF	Not specified	Not economically viable (< 10% IRR)	(Real Guimarães et al., 2023)
Used Tires	Not specified	Gasification Fischer-Tropsch (GFT)	Yes	Aspen Plus®	Yes	Yes	Not specified	Not specified	0.66 USD/L	(Rogachuk & Okolie, 2024)

Used Tires	Not specified	Pyrolysis	Yes	Aspen Plus®	Yes	Yes	Not specified	Not specified	0.78 USD/L	(Rogachuk & Okolie, 2024)
Soybean Oil and Animal Tallow	Brazil	Hydrotreatment (deoxygenation, isomerization, hydrocracking)	Yes	UniSim Design R491	Yes	Yes	Not specified	Not specified	Not specified	(Teixeira et al., 2024)
Ethanol (from corn)	Brazil	Alcohol-to-Jet (ATJ)	Yes	Aspen Plus® v12.1	Yes	No	Not specified	70.0 % GGE[1]/ton of biomass	3.91 USD/GGE**Error! Bookmark not defined.**	(Teixeira et al., 2024)
Ethanol (from corn stover)	Brazil	Alcohol-to-Jet (ATJ)	Yes	Aspen Plus® v12.1	Yes	No	Not specified	49.6 % GGE**Error! Bookmark not defined.**/ton of biomass	5.37 USD/GGE**Error! Bookmark not defined.**	(Teixeira et al., 2024)
Biogas and Corn Stover	Not specified	Hybrid biogas-to-kerosene process	Yes	Aspen Plus® (V12)	Yes	No	Not specified	Not specified	2.78 €2022/kg jetfuel	(Voß et al., 2024)

[1] GGE – gallon gasoline equivalent

Tall Oil Fatty Acid (TOFA)	Not specified	Catalytic deoxygenation (decarboxylation/decarbonylation)	Yes	Aspen Plus®	Yes	Yes	20.8 $gCO_2eq./MJ$	Not specified	0.62 USD/L	(Umenweke et al., 2023)
Tall Oil Fatty Acid (TOFA)	Not specified	Catalytic deoxygenation integrated with hydrothermal gasification for H_2	Yes	Aspen Plus®	Yes	Yes	5.1 $gCO_2eq./MJ$	Not specified	0.39 USD/L	(Umenweke et al., 2023)
Basic Oxygen Furnace Gas (BOFG)	China	Ethanol-to-Jet (ETJ)	Yes	Aspen Plus® (V11)	No	Yes	Emission reduction compared to conventional jet fuel	Not specified	Not specified	(Guo et al., 2024)
Basic Oxygen Furnace Gas (BOFG)	China	Fischer-Tropsch to Jet (FTJ)	Yes	Aspen Plus® (V11)	No	Yes	Emission reduction compared to conventional jet fuel	Not specified	Not specified	(Guo et al., 2024)
Coke Oven Gas (COG)	China	Ethanol-to-Jet (ETJ)	Yes	Aspen Plus® (V11)	No	Yes	Emission reduction compared to conventional jet fuel	Not specified	Not specified	(Guo et al., 2024)
Coke Oven Gas (COG)	China	Fischer-Tropsch to Jet (FTJ)	Yes	Aspen Plus® (V11)	No	Yes	72.76% GHG reduction	Not specified	Not specified	(Guo et al., 2024)

							(23.60 g CO_2eq/MJ)			
(COG + BOFG)	China	Ethanol-to-Jet (ETJ)	Yes	Aspen Plus® (V11)	No	Yes	Emission reduction compared to conventional jet fuel	Not specified	Not specified	(Guo et al., 2024)
(COG + BOFG)	China	Fischer-Tropsch to Jet (FTJ)	Yes	Aspen Plus® (V11)	No	Yes	52.13% GHG reduction (41.48 g CO_2eq/MJ)	Not specified	Not specified	(Guo et al., 2024)
Paper Sludge	USA	Enzymatic hydrolysis, dehydration, aldol condensation, hydroprocessing	Yes	Aspen Plus® (V11)	No	Yes	Minimum GWP of -584 to -925 kgCO_2eq per dry ton of sludge (depending on the scenario)	Not specified	Not specified	(Lan et al., 2024)

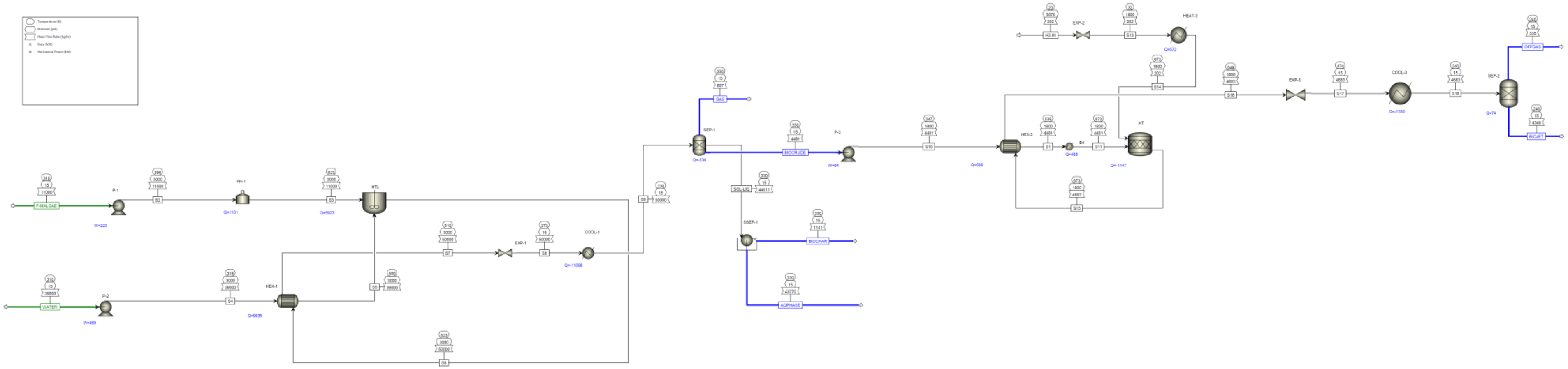

Figure A 1: Preliminary process model flowsheet developed in Aspen Plus® for the HTL pathway. This version also includes a preliminary configuration for the bio-oil upgrading to SAF

Table A 2: Material balances obtained for the preliminary process model in Aspen Plus® for HTL pathway

														Material
Stream Name	**Units**	**AQPHASE**	**BIOCHAR**	**BIOCRUDE**	**BIOJET**	**F-MALGAE**	**GAS**	**H2-IN**	**OFFGAS**	**S1**	**S2**	**S3**	**S4**	**S5**
Description														
From		SSEP-1	SSEP-1	01-Sep	02-Sep		01-Sep		02-Sep	HEX-2	P-1	PH-1	P-2	HEX-1
To				P-3		P-1		EXP-2		B4	PH-1	HTL	HEX-1	HTL
Stream Class		CONVEN	CONVEN	CONVEN	CONVEN	CONVEN	CONVEN	CONVEN	CONVEN	CONVEN	CONVEN	CONVEN	CONVEN	CONVEN
Maximum Relative Error														8.6925E-10
Cost Flow	$/sec													
MIXED Substream														
Phase		Liquid Phase	Solid Phase	Liquid Phase			Vapor Phase	Liquid Phase	Vapor Phase	Liquid Phase			Liquid Phase	Liquid Phase
Temperature	K	329.9999723	330	330	240.15	310.15	330	20.15	240.15	539.2630452	396.3193812	623.15	314.7463002	500.0106744
Pressure	psi	14.50377377	14.50377377	14.50377377	14.50377377	14.7	14.50377377	5076.320821	14.50377377	1800	3000	3000	3000	3000
Molar Vapor Fraction		0	0	0	0.101813201	0	1	0	1	0	0	0	0	0
Molar Liquid Fraction		1	0	1	0.898186799	0.406462554	0	1	0	1	0.406462554	0.406462554	1	1
Molar Solid Fraction		0	1	0	0	0.593537446	0	0	0	0	0.593537446	0.593537446	0	0
Mass Vapor Fraction		0	0	0	0.054907481	0	1	0	1	0	0	0	0	0
Mass Liquid Fraction		1	0	1	0.945092519	0.100010001	0	1	0	1	0.100010001	0.100010001	1	1
Mass Solid Fraction		0	1	0	0	0.899989999	0	0	0	0	0.899989999	0.899989999	0	0
Molar Enthalpy	kJ/kmol	-288976.2413	-628918.9411	-390188.8579	-231210.0505	-199475.2606	-361078.4142	-8227.444711	-27149.79263	-321403.3753	-194123.0195	-167737.4721	-287041.1423	-270519.1079
Mass Enthalpy	kJ/kg	-14536.7343	-10792.42196	-2977.460518	-4125.22106	-2724.400271	-8578.236531	-4081.316701	-2489.500668	-2452.570956	-2651.300243	-2290.930781	-15933.20461	-15016.09233
Molar Entropy	kJ/kmol-K	-165.8529845	-104.9066773	-808.932929	-401.0921051	-85.02533397	7.113790698	-133.7895893	-48.9708895	-655.1629565	-70.51822989	-19.50147836	-166.5888727	-125.4885532
Mass Entropy	kJ/kg-K	-8.343110692	-1.800227429	-6.172820697	-7.15623562	-1.161262014	0.16900423	-66.36783406	-4.490386493	-4.999429882	-0.963126375	-0.266347981	-9.24708762	-6.965673204
Molar Density	kmol/cum	38.07637554	45.27551161	5.037010002	0.478395788	7.379568656	0.036577435	48.355514	0.050300597	4.483711319	7.336704489	6.918678296	41.59346857	33.76816253
Mass Density	kg/cum	756.9215795	2638.3908	660.0877385	26.81308775	540.3175872	1.539631368	97.47891356	0.548564132	587.5793106	537.1791567	506.5720962	749.3179825	608.3429031
Enthalpy Flow	kW	-176742.4265	-3421.667647	-3706.328228	-4982.428906	-8324.556384	-1447.418721	-228.5401309	-231.510936	-3052.94828	-8101.195186	-7000.066275	-172609.7166	-162674.3336
Average MW		19.87903441	58.27412449	131.0475338	56.04791771	73.21804463	42.0923826	2.01588	10.90571816	131.0475338	73.21804463	73.21804463	18.01528	18.01528
Mass Flows	kg/hr	43769.99142	1141.356738	4481.262317	4348.068576	11000	607.4334018	201.588	334.7817417	4481.262317	11000	11000	39000	39000
CELL	kg/hr	0	0.087409072	0	0	891.0891089	0	0	0	0	891.0891089	891.0891089	0	0
PMET	kg/hr	0	0.031519411	0	0	161.1881188	0	0	0	0	161.1881188	161.1881188	0	0
PPHE	kg/hr	0	0.098817612	0	0	505.3465347	0	0	0	0	505.3465347	505.3465347	0	0
PPRO	kg/hr	0	0.157597053	0	0	805.9405941	0	0	0	0	805.9405941	805.9405941	0	0
PASP	kg/hr	0	0.195399049	0	0	999.2574257	0	0	0	0	999.2574257	999.2574257	0	0
PGLY	kg/hr	0	0.31743028	0	0	1623.316832	0	0	0	0	1623.316832	1623.316832	0	0
PSER	kg/hr	0	0.081460639	0	0	416.5841584	0	0	0	0	416.5841584	416.5841584	0	0
PARG	kg/hr	0	0.182620909	0	0	933.9108911	0	0	0	0	933.9108911	933.9108911	0	0
TAG-A-P	kg/hr	0	0.104793241	0	0	469.5544554	0	0	0	0	469.5544554	469.5544554	0	0
TAG-A-S	kg/hr	0	0.33595462	0	0	1505.335534	0	0	0	0	1505.335534	1505.335534	0	0
TAG-A-N	kg/hr	0	0.042370277	0	0	189.8514851	0	0	0	0	189.8514851	189.8514851	0	0
HEXS	kg/hr	0	7.326806732	0	0	44.8019802	0	0	0	0	44.8019802	44.8019802	0	0
PHYTS	kg/hr	0	23.39720603	0	0	143.0693069	0	0	0	0	143.0693069	143.0693069	0	0
CHOLS	kg/hr	0	19.87548124	0	0	121.5346535	0	0	0	0	121.5346535	121.5346535	0	0
ASH	kg/hr	0	1089.108911	0	0	1089.108911	0	0	0	0	1089.108911	1089.108911	0	0
CHAR	kg/hr	0	0.012961119	0	0	0	0	0	0	0	0	0	0	0
GLUC	kg/hr	415.5963197	0	0	0	0	0	0	0	0	0	0	0	0
FRUC	kg/hr	541.7118647	0	0	0	0	0	0	0	0	0	0	0	0
FURF	kg/hr	0	0	0.006582617	0	0	0	0	0	0.006582617	0	0	0	0
5-HMF	kg/hr	0	0	0.008339602	0	0	0	0	0	0.008339602	0	0	0	0
FORM	kg/hr	0	0	0	0	0	18.34045332	0	0	0	0	0	0	0
AACID	kg/hr	0.011758027	0	0	0	0	0	0	0	0	0	0	0	0
CO2	kg/hr	0	0	0	0	0	564.9792455	0	0	0	0	0	0	0
CO	kg/hr	0	0	0	0	0	1.93889E-10	0	0	0	0	0	0	0
CH4	kg/hr	0	0	0	0	0	7.881538642	0	15.76520808	0	0	0	0	0
H2	kg/hr	0	0	0	0	0	0.495183999	201.588	27.98096855	0	0	0	0	0
H2O	kg/hr	38337.74594	0	0	781.5388638	1100.110011	0	0	0	0	1100.110011	1100.110011	39000	39000
MET	kg/hr	0	0	146.6323667	0	0	0	0	0	146.6323667	0	0	0	0
PHE	kg/hr	0	0	63.39267631	0	0	0	0	0	63.39267631	0	0	0	0
PRO	kg/hr	0	0	122.2700317	0	0	0	0	0	122.2700317	0	0	0	0
ASP	kg/hr	438.8619827	0	0	0	0	0	0	0	0	0	0	0	0
GLY	kg/hr	0	0	895.3684289	0	0	0	0	0	895.3684289	0	0	0	0
SER	kg/hr	202.1460147	0	0	0	0	0	0	0	0	0	0	0	0
ARG	kg/hr	834.8510543	0	0	0	0	0	0	0	0	0	0	0	0
SO2	kg/hr	0	0	0	0	0	15.73698032	0	0	0	0	0	0	0
NH3	kg/hr	526.9167979	0	0	0	0	0	0	250.145967	0	0	0	0	0
PYLI	kg/hr	0	0	598.9337179	598.9337179	0	0	0	0	598.9337179	0	0	0	0
PHEA	kg/hr	0	0	39.76574951	0	0	0	0	0	39.76574951	0	0	0	0
GLYA	kg/hr	1302.834707	0	0	0	0	0	0	0	0	0	0	0	0
MALA	kg/hr	721.8880402	0	0	0	0	0	0	0	0	0	0	0	0

Stream Name	**S6**	**S7**	**S8**	**S9**	**S10**	**S11**	**S13**	**S14**	**S15**	**S16**	**S17**	**S18**	**SOL-LIQ**	**WATER**
Description														
From	HTL	HEX-1	EXP-1	COOL-1	P-3	B4	EXP-2	HEAT-3	HT	HEX-2	EXP-3	COOL-3	01-Sep	
To	HEX-1	EXP-1	COOL-1	01-Sep	HEX-2	HT	HEAT-3	HT	HEX-2	EXP-3	COOL-3	02-Sep	SSEP-1	P-2
Stream Class	CONVEN	CONVEN	CONVEN	CONVEN	CONVEN	CONVEN	CONVEN	CONVEN	CONVEN	CONVEN	CONVEN	CONVEN	CONVEN	CONVEN
Maximum Relative Error														
Cost Flow														
MIXED Substream														
Phase					Liquid Phase	Liquid Phase	Liquid Phase	Liquid Phase	Vapor Phase					Liquid Phase
Temperature	623.15	510.0016439	373.1627943	330	346.7423935	673.15	31.60775255	673.15	673.15	549.2679381	474.4849815	240.15	330	310.15
Pressure	3000	3000	14.50377377	14.50377377	1800	1800	1800	1800	1800	1800	14.50377377	14.50377377	14.50377377	14.50377377
Molar Vapor Fraction	0.133032001	0.004132225	0.335419561	0.013977475	0	0	0	0	1	0.537098488	0.964361297	0.266361046	0	0
Molar Liquid Fraction	0.858339919	0.987239695	0.655952359	0.977394445	1	1	1	1	0	0.462901512	0.035638703	0.733638954	0.991183051	1
Molar Solid Fraction	0.00862808	0.00862808	0.00862808	0.00862808	0	0	0	0	0	0	0	0	0.008816949	0
Mass Vapor Fraction	0.165659137	0.046998856	0.347429686	0.067537719	0	0	0	0	1	0.343788103	0.786285733	0.093732536	0	0
Mass Liquid Fraction	0.811513749	0.930174029	0.6297432	0.909635166	1	1	1	1	0	0.656211897	0.213714267	0.906267464	0.974586451	1
Mass Solid Fraction	0.022827115	0.022827115	0.022827115	0.022827115	0	0	0	0	0	0	0	0	0.025413549	0
Molar Enthalpy	-259690.1364	-275446.4866	-275446.487	-293042.7474	-383425.1522	-270036.0494	-8227.444711	12351.05214	-112024.5284	-131612.3188	-131612.3188	-175825.2639	-291973.4988	-287820.8466
Mass Enthalpy	-11790.0747	-12505.42164	-12505.42166	-13304.30153	-2925.847905	-2060.596194	-4081.316701	6126.878651	-2590.198913	-3043.102168	-3043.102168	-4065.381164	-14441.57803	-15976.48477
Molar Entropy	-103.8433162	-131.4275992	-123.8209918	-172.0226228	-796.16842	-570.2761216	-114.005371	-31.68052565	-175.1507721	-207.4305967	-172.5098614	-307.9946811	-165.3156166	-167.5003681
Mass Entropy	-4.71454354	-5.966885121	-5.621540975	-7.809921469	-6.07541704	-4.351673816	-56.55364954	-15.7154819	-4.049785757	-4.796150573	-3.988723381	-7.1213644	-8.176832441	-9.297683305
Molar Density	17.27987236	16.20579053	0.096845698	2.613870774	5.032980479	3.875416298	38.65387292	11.2731252	2.500599712	3.950561579	0.026389481	0.186480512	38.12983117	41.58945126
Mass Density	380.6093283	356.9514243	2.133139375	57.57355025	659.5596795	507.8637484	77.92156935	22.72526762	108.1494174	170.8593867	1.141328997	8.065168759	770.8922246	749.2456094
Enthalpy Flow	-163751.1812	-173686.5641	-173686.5643	-184782.1279	-3642.0811	-2565.020021	-228.5401309	343.0847815	-3369.309389	-3958.442209	-3958.442209	-5288.214298	-180164.0942	-173078.585
Average MW	22.02616549	22.02616549	22.02616549	22.02616549	131.0475338	131.0475338	2.01588	2.01588	43.24939209	43.24939209	43.24939209	43.24939209	20.21756197	18.01528
Mass Flows	50000.04388	50000.04388	50000.04388	50000.04388	4481.262317	4481.262317	201.588	201.588	4682.850317	4682.850317	4682.850317	4682.850317	44911.34816	39000
CELL	0.087409072	0.087409072	0.087409072	0.087409072	0	0	0	0	0	0	0	0	0.087409072	0
PMET	0.031519411	0.031519411	0.031519411	0.031519411	0	0	0	0	0	0	0	0	0.031519411	0
PPHE	0.098817612	0.098817612	0.098817612	0.098817612	0	0	0	0	0	0	0	0	0.098817612	0
PPRO	0.157597053	0.157597053	0.157597053	0.157597053	0	0	0	0	0	0	0	0	0.157597053	0
PASP	0.195399049	0.195399049	0.195399049	0.195399049	0	0	0	0	0	0	0	0	0.195399049	0
PGLY	0.31743028	0.31743028	0.31743028	0.31743028	0	0	0	0	0	0	0	0	0.31743028	0
PSER	0.081460639	0.081460639	0.081460639	0.081460639	0	0	0	0	0	0	0	0	0.081460639	0
PARG	0.182620909	0.182620909	0.182620909	0.182620909	0	0	0	0	0	0	0	0	0.182620909	0
TAG-A-P	0.104793241	0.104793241	0.104793241	0.104793241	0	0	0	0	0	0	0	0	0.104793241	0
TAG-A-S	0.33595462	0.33595462	0.33595462	0.33595462	0	0	0	0	0	0	0	0	0.33595462	0
TAG-A-N	0.042370277	0.042370277	0.042370277	0.042370277	0	0	0	0	0	0	0	0	0.042370277	0
HEXS	7.326806732	7.326806732	7.326806732	7.326806732	0	0	0	0	0	0	0	0	7.326806732	0
PHYTS	23.39720603	23.39720603	23.39720603	23.39720603	0	0	0	0	0	0	0	0	23.39720603	0
CHOLS	19.87548124	19.87548124	19.87548124	19.87548124	0	0	0	0	0	0	0	0	19.87548124	0
ASH	1089.108911	1089.108911	1089.108911	1089.108911	0	0	0	0	0	0	0	0	1089.108911	0
CHAR	0.012961119	0.012961119	0.012961119	0.012961119	0	0	0	0	0	0	0	0	0.012961119	0
GLUC	415.5963197	415.5963197	415.5963197	415.5963197	0	0	0	0	0	0	0	0	415.5963197	0
FRUC	541.7118647	541.7118647	541.7118647	541.7118647	0	0	0	0	0	0	0	0	541.7118647	0
FURF	0.006582617	0.006582617	0.006582617	0.006582617	0.006582617	0.006582617	0	0	0	0	0	0	0	0
5-HMF	0.008339602	0.008339602	0.008339602	0.008339602	0.008339602	0.008339602	0	0	0	0	0	0	0	0
FORM	18.34045332	18.34045332	18.34045332	18.34045332	0	0	0	0	0	0	0	0	0	0
AACID	0.011758027	0.011758027	0.011758027	0.011758027	0	0	0	0	0	0	0	0	0.011758027	0
CO2	564.9792455	564.9792455	564.9792455	564.9792455	0	0	0	0	0	0	0	0	0	0
CO	1.93889E-10	1.93889E-10	1.93889E-10	1.93889E-10	0	0	0	0	0	0	0	0	0	0
CH4	7.881538642	7.881538642	7.881538642	7.881538642	0	0	0	0	15.76520808	15.76520808	15.76520808	15.76520808	0	0
H2	0.495183999	0.495183999	0.495183999	0.495183999	0	0	201.588	201.588	27.98096855	27.98096855	27.98096855	27.98096855	0	0
H2O	38337.74594	38337.74594	38337.74594	38337.74594	0	0	0	0	781.5388638	781.5388638	781.5388638	781.5388638	38337.74594	39000
MET	146.6323667	146.6323667	146.6323667	146.6323667	146.6323667	146.6323667	0	0	0	0	0	0	0	0
PHE	63.39267631	63.39267631	63.39267631	63.39267631	63.39267631	63.39267631	0	0	0	0	0	0	0	0
PRO	122.2700317	122.2700317	122.2700317	122.2700317	122.2700317	122.2700317	0	0	0	0	0	0	0	0
ASP	438.8619827	438.8619827	438.8619827	438.8619827	0	0	0	0	0	0	0	0	438.8619827	0
GLY	895.3684289	895.3684289	895.3684289	895.3684289	895.3684289	895.3684289	0	0	0	0	0	0	0	0
SER	202.1460147	202.1460147	202.1460147	202.1460147	0	0	0	0	0	0	0	0	202.1460147	0
ARG	834.8510543	834.8510543	834.8510543	834.8510543	0	0	0	0	0	0	0	0	834.8510543	0
SO2	15.73698032	15.73698032	15.73698032	15.73698032	0	0	0	0	0	0	0	0	0	0
NH3	526.9167979	526.9167979	526.9167979	526.9167979	0	0	0	0	250.145967	250.145967	250.145967	250.145967	526.9167979	0
PYLI	598.9337179	598.9337179	598.9337179	598.9337179	598.9337179	598.9337179	0	0	598.9337179	598.9337179	598.9337179	598.9337179	0	0
PHEA	39.76574951	39.76574951	39.76574951	39.76574951	39.76574951	39.76574951	0	0	0	0	0	0	0	0
GLYA	1302.834707	1302.834707	1302.834707	1302.834707	0	0	0	0	0	0	0	0	1302.834707	0
MALA	721.8880402	721.8880402	721.8880402	721.8880402	0	0	0	0	0	0	0	0	721.8880402	0

PYRA	kg/hr	219.6800759	0	0	0	0	0	0	0	0	0	0	0	0	219.6800759	219.6800759	219.6800759	219.6800759	0	0	0	0	0	0	0	0	219.6800759	0
STYR	kg/hr	0	0	283.399887	0	0	0	0	0	283.399887	0	0	0	0	283.399887	283.399887	283.399887	283.399887	283.399887	283.399887	0	0	0	0	0	0	0	0
1E2PYR	kg/hr	0	0	1.65829E-05	0	0	0	0	0	1.65829E-05	0	0	0	0	1.65829E-05	1.65829E-05	1.65829E-05	1.65829E-05	1.65829E-05	1.65829E-05	0	0	0	0	0	0	0	0
METPYR	kg/hr	0	0	14.68666815	0	0	0	0	0	14.68666815	0	0	0	0	14.68666815	14.68666815	14.68666815	14.68666815	14.68666815	14.68666815	0	0	0	0	0	0	0	0
INDOLE	kg/hr	0	0	0.000824039	0	0	0	0	0	0.000824039	0	0	0	0	0.000824039	0.000824039	0.000824039	0.000824039	0.000824039	0.000824039	0	0	8.24039E-11	8.24039E-11	8.24039E-11	8.24039E-11	0	0
PALA	kg/hr	0	0	429.7741792	0	0	0	0	0	429.7741792	0	0	0	0	429.7741792	429.7741792	429.7741792	429.7741792	429.7741792	429.7741792	0	0	0	0	0	0	0	0
STEA	kg/hr	0	0	1412.448336	0	0	0	0	0	1412.448336	0	0	0	0	1412.448336	1412.448336	1412.448336	1412.448336	1412.448336	1412.448336	0	0	0	0	0	0	0	0
NONA	kg/hr	0	0	182.0713048	0	0	0	0	0	182.0713048	0	0	0	0	182.0713048	182.0713048	182.0713048	182.0713048	182.0713048	182.0713048	0	0	0	0	0	0	0	0
GLYC	kg/hr	227.7468726	0	0	0	0	0	0	0	0	0	0	0	0	227.7468726	227.7468726	227.7468726	227.7468726	0	0	0	0	0	0	0	0	227.7468726	0
C16AMIDE	kg/hr	0	0	17.48341328	0	0	0	0	0	17.48341328	0	0	0	0	17.48341328	17.48341328	17.48341328	17.48341328	17.48341328	17.48341328	0	0	0	0	0	0	0	0
C18AMIDE	kg/hr	0	0	28.22018205	0	0	0	0	0	28.22018205	0	0	0	0	28.22018205	28.22018205	28.22018205	28.22018205	28.22018205	28.22018205	0	0	0	0	0	0	0	0
HEX	kg/hr	0	0	37.47517347	37.47517347	0	0	0	0	37.47517347	0	0	0	0	37.47517347	37.47517347	37.47517347	37.47517347	37.47517347	37.47517347	0	0	37.47517347	37.47517347	37.47517347	37.47517347	0	0
NPHYT	kg/hr	0	0	112.4017555	112.4017555	0	0	0	0	112.4017555	0	0	0	0	112.4017555	112.4017555	112.4017555	112.4017555	112.4017555	112.4017555	0	0	112.4017555	112.4017555	112.4017555	112.4017555	0	0
CHOL	kg/hr	0	0	96.92268361	96.92268361	0	0	0	0	96.92268361	0	0	0	0	96.92268361	96.92268361	96.92268361	96.92268361	96.92268361	96.92268361	0	0	96.92268361	96.92268361	96.92268361	96.92268361	0	0
BUTANE	kg/hr	0	0	0	57.11782108	0	0	0	0	0	0	0	0	0	0	0	0	0	0	0	0	0	57.11782108	57.11782108	57.11782108	57.11782108	0	0
ETHANE	kg/hr	0	0	0	358.6572028	0	0	0	0	0	0	0	0	0	0	0	0	0	0	0	0	0	358.6572028	358.6572028	358.6572028	358.6572028	0	0
H2S	kg/hr	0	0	0	0	0	0	0	33.49223762	0	0	0	0	0	0	0	0	0	0	0	0	0	33.49223762	33.49223762	33.49223762	33.49223762	0	0
NPROPBEZ	kg/hr	0	0	0	46.12476767	0	0	0	0	0	0	0	0	0	0	0	0	0	0	0	0	0	46.12476767	46.12476767	46.12476767	46.12476767	0	0
PENTANE	kg/hr	0	0	0	76.62350193	0	0	0	0	0	0	0	0	0	0	0	0	0	0	0	0	0	76.62350193	76.62350193	76.62350193	76.62350193	0	0
PROPANE	kg/hr	0	0	0	0	0	0	0	0	0	0	0	0	0	0	0	0	0	0	0	0	0	0	0	0	0	0	0
2MFURAN	kg/hr	0	0	0	0.005624636	0	0	0	0	0	0	0	0	0	0	0	0	0	0	0	0	0	0.005624636	0.005624636	0.005624636	0.005624636	0	0
2-MET-01	kg/hr	0	0	0	0	0	0	0	0	0	0	0	0	0	0	0	0	0	0	0	0	0	0	0	0	0	0	0
METHA-01	kg/hr	0	0	0	0	0	0	0	0	0	0	0	0	0	0	0	0	0	0	0	0	0	0	0	0	0	0	0
HYDRAZIN	kg/hr	0	0	0	0	0	0	0	0	0	0	0	0	0	0	0	0	0	0	0	0	0	0	0	0	0	0	0
PPDINE	kg/hr	0	0	0	0	0	0	0	0	0	0	0	0	0	0	0	0	0	0	0	0	0	0	0	0	0	0	0
ETHYLAMI	kg/hr	0	0	0	0	0	0	0	7.397287601	0	0	0	0	0	0	0	0	0	0	0	0	0	7.397287601	7.397287601	7.397287601	7.397287601	0	0
PHENAMI	kg/hr	0	0	0	0	0	0	0	0	0	0	0	0	0	0	0	0	0	0	0	0	0	0	0	0	0	0	0
ETHYLBEN	kg/hr	0	0	0	306.3045166	0	0	0	0	0	0	0	0	0	0	0	0	0	0	0	0	0	306.3045166	306.3045166	306.3045166	306.3045166	0	0
1EPPDINE	kg/hr	0	0	0	1.45337E-05	0	0	0	0	0	0	0	0	0	0	0	0	0	0	0	0	0	1.45337E-05	1.45337E-05	1.45337E-05	1.45337E-05	0	0
METPYRA	kg/hr	0	0	0	15.41663706	0	0	0	0	0	0	0	0	0	0	0	0	0	0	0	0	0	15.41663706	15.41663706	15.41663706	15.41663706	0	0
BENZENE	kg/hr	0	0	0	12.81663028	0	0	0	0	0	0	0	0	0	0	0	0	0	0	0	0	0	12.81663028	12.81663028	12.81663028	12.81663028	0	0
TOLUENE	kg/hr	0	0	0	0.00021604	0	0	0	0	0	0	0	0	0	0	0	0	0	0	0	0	0	0.00021604	0.00021604	0.00021604	0.00021604	0	0
N-HEX-01	kg/hr	0	0	0	395.0215621	0	0	0	0	0	0	0	0	0	0	0	0	0	0	0	0	0	395.0215621	395.0215621	395.0215621	395.0215621	0	0
N-OCT-01	kg/hr	0	0	0	1288.917598	0	0	0	0	0	0	0	0	0	0	0	0	0	0	0	0	0	1288.917598	1288.917598	1288.917598	1288.917598	0	0
N-NON-01	kg/hr	0	0	0	163.7836824	0	0	0	0	0	0	0	0	0	0	0	0	0	0	0	0	0	163.7836824	163.7836824	163.7836824	163.7836824	0	0
SORBITOL	kg/hr	0	0	0	0	0	0	0	0	0	0	0	0	0	0	0	0	0	0	0	0	0	0	0	0	0	0	0
S	kg/hr	0	0	0	0	0	0	0	0	0	0	0	0	0	0	0	0	0	0	0	0	0	0	0	0	0	0	0
METHAMI	kg/hr	0	0	0	0	0	0	0	7.28196E-05	0	0	0	0	0	0	0	0	0	0	0	0	0	7.28196E-05	7.28196E-05	7.28196E-05	7.28196E-05	0	0
2:4-D-01	kg/hr	0	0	0	0.006356873	0	0	0	0	0	0	0	0	0	0	0	0	0	0	0	0	0	0.006356873	0.006356873	0.006356873	0.006356873	0	0
O-XYL-01	kg/hr	0	0	0	0.000248928	0	0	0	0	0	0	0	0	0	0	0	0	0	0	0	0	0	0.000248928	0.000248928	0.000248928	0.000248928	0	0
Volume Flow	l/hr	57826.32258	432.5957846	6788.888895	162162.1731	20358.3971	394531.7134	2068.016483	610287.3345	7626.650966	20477.33957	21714.57939	52047.32958	64108.58054	131368.4142	140075.2049	23439651.65	868455.1093	6794.324239	8823.749149	2587.062885	8870.654611	43299.8201	27407.62687	4102980.236	580626.4515	58258.91964	52052.35708
Heat capacity, mixture	kJ/kmol-K	89.47549399	46.84323727	276.7683701	123.6594928	47.42789631	38.68345067	32.11004807	31.8703021	360.227433	73.70346954	186.6404659	86.10896506	97.25732631	202.4479827	105.92874	74.91862964	91.23787504	282.4161456	408.1835034	35.20027501	31.73355427	143.9585545	156.5139075	101.7315151	101.5447925	89.09960788	86.68140514
Enthalpy, mixture	kJ/kmol	-288976.2413	-628918.9411	-390188.8579	-231210.0505	-199475.2606	-361078.4142	-8227.444711	-27149.79263	-321403.3753	-194123.0195	-167737.4721	-287041.1423	-270519.1079	-259690.1364	-275446.4866	-275446.487	-293042.7474	-383425.1522	-270036.0494	-8227.444711	12351.05214	-112024.5284	-131612.3188	-131612.3188	-175825.2639	-291973.4988	-287820.8466
Internal energy, mixture	kJ/kmol	-288978.8701	-628921.1496	-390208.711	-231419.0825	-199488.9949	-363812.3402	-8951.25048	-29137.84061	-324171.2973	-196942.3034	-170727.0998	-287538.4384	-271131.6456	-260887.1518	-276722.8373	-276479.0573	-293081.0048	-385890.9999	-273238.4313	-8548.513578	11250.15394	-116987.5631	-134753.7672	-135401.7076	-176361.513	-291976.1214	-287823.251
Molecular weight, mixture		19.87903441	58.27412449	131.0475338	56.04791771	73.21804463	42.0923826	2.01588	10.90571816	131.0475338	73.21804463	73.21804463	18.01528	18.01528	22.02616549	22.02616549	22.02616549	22.02616549	131.0475338	131.0475338	2.01588	2.01588	43.24939209	43.24939209	43.24939209	43.24939209	20.21756197	18.01528
Vapor Phase																												
Molar Enthalpy	kJ/kmol				-88688.69082		-361078.4142		-27149.79263						-253361.8842	-543696.0613	-237117.7371	-361357.3508					-112024.5284	-112620.4592	-124175.1454	-41976.67204		
Mass Enthalpy	kJ/kg				-2934.143361		-8578.236531		-2489.500668						-9237.258823	-2170.27106	-10393.13591	-3395.317113					-2590.198913	-4068.181988	-3521.38935	-2758.089401		
Molar Entropy	kJ/kmol-K				-184.7051888		7.113790698		-48.9708895						-118.0259362	-1172.228029	-55.78483941	-425.6039875					-175.1507721	-125.9785057	-128.1931678	-75.13308112		
Mass Entropy	kJ/kg-K				-6.110717143		0.16900423		-4.490386493						-4.303078675	-4.679181528	-2.445111972	-3.998979125					-4.049785757	-4.550713886	-3.635333419	-4.936640868		
Molar Density	kmol/cum				0.050821519		0.036577435		0.050300597						9.82339698	0.147895891	0.032543877	0.039281122					2.500599712	3.380397965	0.025462012	0.050277672		
Mass Density	kg/cum				1.536153287		1.539631368		0.548564132						269.4386306	37.05086191	0.742483365	4.180617537					108.1494174	93.58036893	0.89786977	0.765199763		
Enthalpy Flow	kW				-194.5838251		-1447.418721		-231.510936						-21253.30089	-1416.671477	-50151.20987	-3184.891309					-3369.309389	-1819.277683	-3601.655895	-336.2842159		
Average MW					30.22643406		42.0923826		10.90571816						27.42825432	250.5198873	22.81484041	106.4281593					43.24939209	27.68324022	35.26311153	15.21947477		
Volume Flow	l/hr				155415.1504		394531.7134		610287.3345						30741.561	63424.83649	23396483.13	807748.8269					43299.8201	17203.48239	4100882.467	573622.0245		
Heat capacity, mixture	kJ/kmol-K				48.13098322		38.68345067		31.8703021						235.4220034	547.679268	41.72966747	161.4250963					143.9585545	94.74568911	79.69122174	36.77257781		
Enthalpy, mixture	kJ/kmol				-88688.69082		-361078.4142		-27149.79263						-253361.8842	-543696.0613	-237117.7371	-361357.3508					-112024.5284	-112620.4592	-124175.1454	-41976.67204		
Internal energy, mixture	kJ/kmol				-90656.36125		-363812.3402		-29137.84061						-255467.4971	-683553.0361	-240190.5117	-363903.1029					-116987.5631	-116291.7912	-128102.5648	-43965.62649		
Molecular weight, mixture					30.22643406		42.0923826		10.90571816						27.42825432	250.5198873	22.81484041	106.4281593					43.24939209	27.68324022	35.26311153	15.21947477		